NARROW FREQUENCY-BAND LASER WITH OPTICAL FEEDBACK

by

MICHAEL J. CHILDRESS

Submitted to the Department of Physics in partial fulfillment of the Requirements for the Degree of

BACHELOR OF SCIENCE

at the

MASSACHUSETTS INSTITUTE OF TECHNOLOGY

June, 2005

Signature of Author _____

Department of Physics
May 6, 2005

Certified by _____

Professor Vladan Vuletic
Thesis Supervisor, Department of Physics

_____

James K. Thompson, Co-Supervisor

Accepted by _____

Professor David Pritchard
Senior Thesis Coordinator, Department of Physics

Narrow Frequency-Band Laser with Optical Feedback

Michael J. Childress

Massachusetts Institute of Technology
Department of Physics

May 5, 2005

Abstract

In this paper we discuss the construction of a narrow frequency-band laser with optical feedback. We use a distributed Bragg reflector (DBR) laser diode centered at the cesium D_2 transition wavelength, $\lambda = 852$ nm. The linewidth of this diode is reduced by several orders of magnitude by means of optical feedback from an external cavity. The system is further stabilized by locking the path length between diode and cavity to optimize coupling between them. The absolute frequency of our laser is fixed by means of a delay line lock system that uses the beat note between our laser and a fixed reference laser to set our laser's frequency. We present both the theory behind these systems and data from our own setup. We then finally discuss potential uses of the narrow laser in atomic physics experiments, including detection of a single atom in an optical cavity.

1 Introduction

The central objective of this project was to construct a narrow frequency-band laser whose linewidth is significantly reduced by means of external optical feedback. Such a laser is useful in conducting high precision atomic physics experiments because it is highly stable and very precise in frequency.

The primary mechanism for achieving a narrow linewidth of our laser is through the use of optical feedback from an external cavity. We use a distributed Bragg

reflector (DBR) laser diode, described in Section 3, operating at $\lambda = 852$ nm. This wavelength corresponds to the cesium D_2 transition, which is described in detail in Section 2. A portion of the laser light from our diode is picked off by means of beamsplitting glass and is sent to the external cavity, while the remainder of the laser light goes on to an optical isolator to be used in experimental setups.

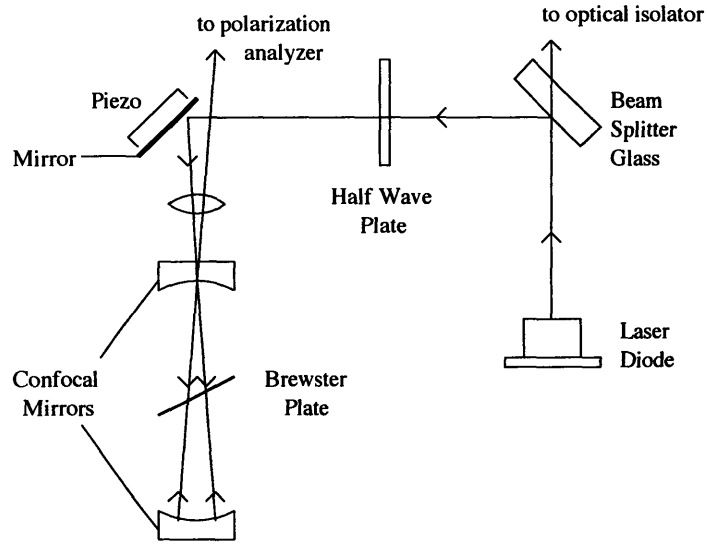

Figure 1: Arrangement of laser and feedback optics.

The light picked off at the BS glass is coupled into a confocal $L = 10$ cm cavity in a V-mode (see Figure 1) so that the resonant cavity output from one branch of the V-mode reflects exactly along the incident path and returns to the laser diode. The effect of this external feedback is that the linewidth of the diode output is dramatically narrowed. In a similar setup, Dahmani [2] uses semiconductor laser diodes with unperturbed linewidths on the order of $\Gamma_{las} \sim 20 - 50$ MHz coupled to cavities with cavity linewidths ranging from $\Gamma_{cav} = 4 - 75$ MHz to produce narrowed laser linewidths of $\Gamma_{nar} \sim 20$ KHz. Thus this scheme can reduce laser linewidths by factors of up to 10^3, even reducing the linewidth below the natural linewidth of our optical transitions. This allows for use in experiments where precise transitions are required, as will be discussed further in Section 9.

Optimum feedback is achieved when the path length between the laser diode and the cavity is equal to an integral number of wavelengths. This is true because this condition allows for optimum coupling of the cavity to the laser diode, as will be discussed further in Section 7. To achieve this condition, the second output beam of the cavity V-mode is sent to a polarization analysis box, and the error signal from

this box is fed back with some gain to a piezo that can be used to optimize the path length.

Once the path length has been locked, the laser is essentially pulled to a wavelength that is resonant with the cavity, but because of the thermal expansion of the cavity and the fact that many wavelengths are resonant with the same cavity length, it becomes necessary to lock the frequency of the laser to the exact frequency desired for experimental use. To accomplish this, we pick off a portion of the light beyond the optical isolator and overlap this light with a reference laser. The beat note from this overlap is sent to a delay line lock system similar to that proposed by Schunemann et al [4]. Our scheme for obtaining an error for this system is described in detail in Section 8, and the error signal from this system is fed back to a piezo on the cavity to optimize the cavity length.

2 Optical Transitions in Atomic Cesium

The primary motivation for the construction of our narrow laser system is for use in experiments in which the laser will drive optical transitions in cold cesium atoms. In particular, we will use the laser to drive the transition between the $6^2S_{1/2}$ and $6^2P_{3/2}$ levels, a transition commonly referred to as the cesium D_2 transition [3]. This transition has a wavelength of $\lambda \approx 852$ nm, with small variations (on the order of $\sim 10^{-5}$) for the different hyperfine transitions, and a natural linewidth of $\Gamma = 2\pi \times 5.22$ MHz. Cesium has nuclear spin $I = 7/2$ so the $6^2S_{1/2}$ level has two hyperfine states, $F = 3, 4$, while the $6^2P_{3/2}$ level has $F = 2, 3, 4, 5$ hyperfine levels. The energy level diagram of this transition is depicted in Figure 2, and the primary transition line we want to set our laser to is the $F = 3 \rightarrow F = 2$ transition at $\lambda = 852.336$ nm.

From this diagram we can establish several criteria which our laser should satisfy. Firstly, in order to be able to drive all possible transitions of the D_2 line, our laser should be tunable over several angstroms. Thus we have chosen for our system a distributed Bragg reflector (DBR) semiconductor laser diode. This DBR, a specialized type of distributed feedback (DFB) laser diode, gives the desired tunability and is discussed further in Section 3.

The linewidth of a standard broad laser is typically on the order of ~ 10 MHz, while the linewidth of the D_2 transition is about ~ 5 MHz. The consequence of this is that some of the photons in our laser beam will have energies that are not resonant with the D_2 transition. For a narrow laser, however, we can reduce the laser linewidth

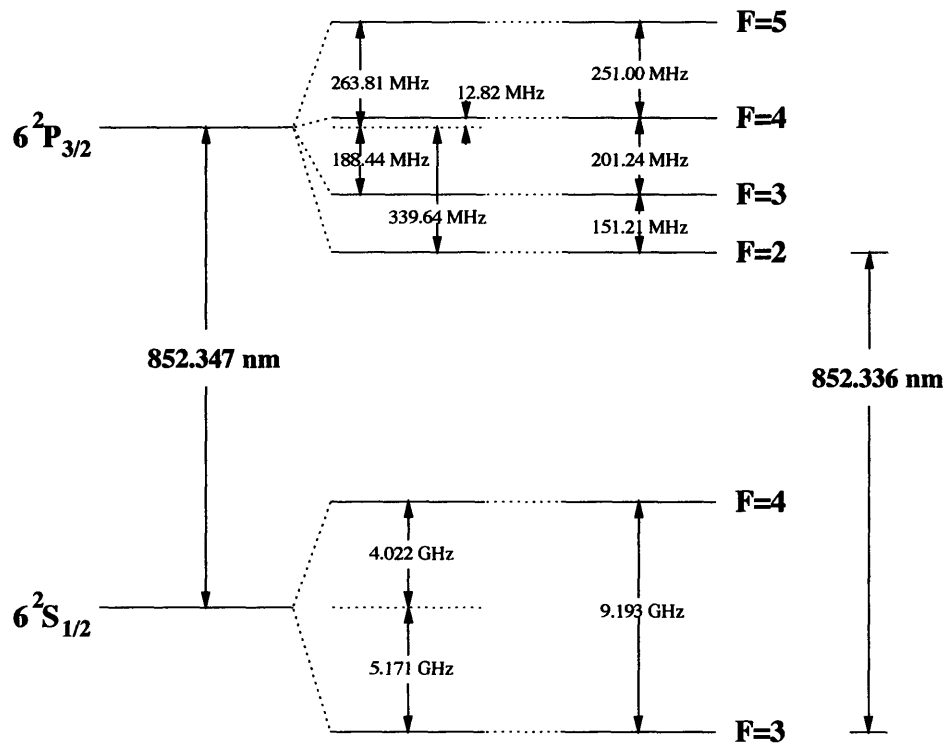

Figure 2: Atomic energy level diagram for the Cesium D_2 transition line. Figure is simplied version of Figure 2 from Los Alamos data [3].

to $\Gamma_{narrow} \sim 10$ kHz. This ensures that all of the photons emitted by our laser will be resonant with the desired cesium transition.

3 DBR Laser Diode

The laser diode used in this setup is a distributed Bragg reflector (DBR) semiconductor laser diode whose central wavelength is $\lambda \approx 850$ nm. The DBR laser diode is a special subset of a larger class of laser diodes known as distributed feedback (DFB) laser diodes. DFB laser diodes consist of multiple semiconductor layers of differing indices of refraction n_i, with the interface between two of the layers having a corrugated shape, as depicted in Figure 3. The n_2 layer is periodic with physical separation Λ between adjacent lattice sites. Light in the laser diode cavity undergoes multiple coherent scatterings from the periodic dielectric interface unless its wavelength is equal to twice the interface spacing. This scattering process in the diode cavity essentially pulls the laser wavelength to the free space Bragg wavelength λ_b, which is related to

the lattice spacing by:

$$\frac{\lambda_b}{n_{eff}} = 2\Lambda \tag{1}$$

where n_{eff} is the effective refractive index of the propogating medium. The right hand side of the previous equation is required to satisfy the Bragg scattering condition, while the equality is required to maintain a constant laser frequency. This equation assumes a first order lattice mode, that is a mode in which $\lambda_b = 2n_{eff}\Lambda$. For free space wavelengths of order $\sim$ 1000nm and real n values of order $\sim$ 2, this requires lattice spacing on the order of a few tenths of a micron.

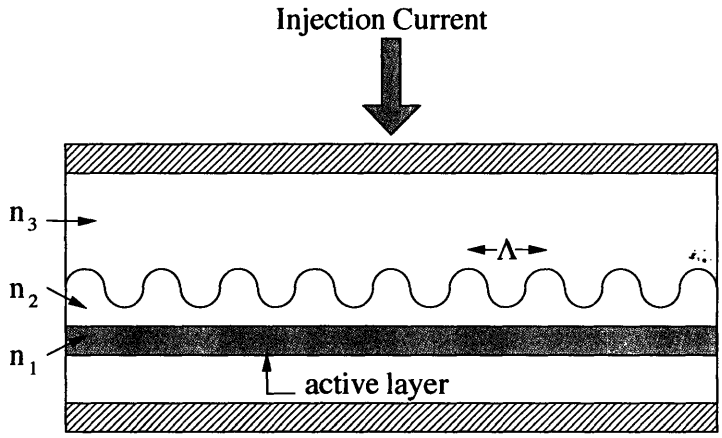

Figure 3: Physical structure of distributed feedback laser diodes. Figure is adapted from Ghafouri-Shiraz Figure 2.8 [5].

The DFB laser wavelength is tuned by varying n_{eff} using the injection current. The injection current alters the semiconductor index of refraction by changing the density of free charge carriers (this is known as the free plasma effect [5]). The main drawback to standard DFB laser diodes is that the tuning range is often very small, typically on the order of a few angstroms for laser wavelengths on the order of $\sim$ 1000nm. This is because the injection current cannot be tuned over a very large range since it also controls the active region.

One scheme for increasing the tunability of DFB diodes involves the introduction of a phase-controlled region. The current passing through this region is controlled separately from the injection current sent through the active lasing region. A phase-controlled region placed between two passive Bragg reflector regions then introduces new boundary conditions for the light field at each of the interfaces. This then changes the resonance conditions which in turns changes the wavelength selected by the laser

diode. In addition, a phase controlled region following an active region acts as an extension of the laser diode cavity, allowing a shorter active diode cavity to act as a longer cavity. It has been demonstrated [5] that the introduction of such a region can greatly increase the tuning range of DFB laser diodes.

Distributed Bragg reflector (DBR) laser diodes are capable of tuning over much larger ranges than standard DFBs because they separate the active region from the Bragg feedback region, as depicted in Figure 4. A typical DBR laser diode consists of three stages: an active region in which lasing is initiated by the injection current, a phase-controlled region used for added tunability, and a passive Bragg reflector region controlled by a tuning current.

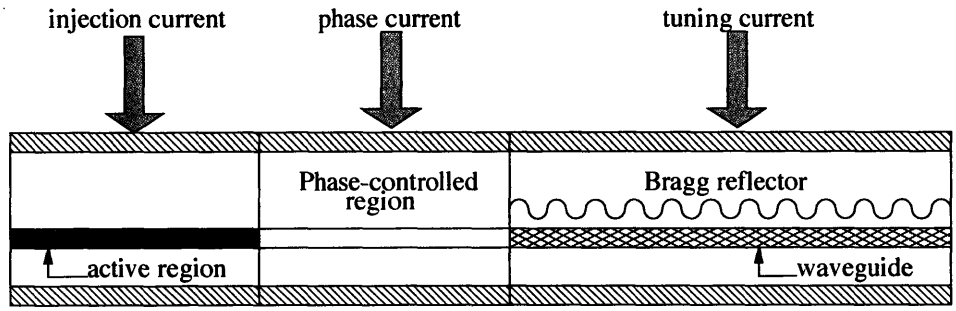

Figure 4: Physical structure of a three stage DBR laser diode. Figure is adapted from Ghafouri-Shiraz Figure 10.21 [5].

The passive DBR region performs the same role as the Bragg lattice of a standard DFB laser diode, but its separation from the active region allows for a greater range of possible tuning currents. This therefore gives us a wider range of Bragg wavelengths that can be passed through the DBR region. Here the phase-controlled region not only serves to extend the diode cavity, but also controls the coupling of the active region to the passive Bragg reflector region. The added tunability from the Bragg reflector region in conjunction with the additional range provided by the phase-controlled region make the wavelength tuning range of a typical DBR laser diode much great than that of a standard DFB laser diode. Typical DBR laser diodes can tune over a range of several nanometers, a full order of magnitude greater than that of standard DFBs.

A major limitation of DBR laser diodes is that the feedback from the Bragg reflector region is quite poor, because the Bragg region is not a very high quality optical structure. The primary role of the Bragg reflector then is wavelength selectivity. Because of the highly nonlinear gain properties of semiconductor laser diodes, even

the poor selectivity of the Bragg reflector provides enough gain imbalance to pull the laser wavelength to that of the passive Bragg reflector region. Because of the poor quality of the Bragg reflector, mode hopping occurs much more frequently in a DBR laser diode than in a standard laser diode. An additional negative consequence of the Bragg reflector's poor quality is that the linewidth of a DBR is somewhat broad ($\sim$ 10MHz). To achieve a narrower linewidth, we need feedback from a higher finesse optical filter. It is for this reason that we choose to use external feedback from an optical cavity.

4 Cavity Dynamics

Our external optical cavity consists of two spherical mirrors separated by a distance $L = 10$ cm equal to the mirrors' radius of curvature. This confocal arrangement has degenerate transverse modes, which is crucial to our setup because this condition allows for us to create the desired V-mode in our cavity. To provide stronger feedback, the reflectivity of the back mirror is higher than that of the front mirror, so that most of the light exiting the cavity does so through the front. Specifically, the mirror power transmission coefficients are $T_F = 0.016$ for the front mirror and $T_B = 2 \times 10^{-5}$ for the back mirror.

The cavity then becomes a Fabry-Perot interferometer and can be treated as a passive optical filter with a frequency gain profile given by:

$$g_{cav}(\omega) = \frac{R_B R T_F^2}{(1-R^2)^2} \frac{1}{1 + \frac{4R^2}{(1-R^2)^2} \sin^2(2\omega L/c)} \tag{2}$$

where R_B is the reflectivity of the back mirror, $R = \sqrt{R_F R_B}$ is the geometric averaged mirror reflectivity, and $\omega = 2\pi c/\lambda$ is the frequency of the light [7]. The above equation differs from that given in [7] because in our setup we want to analyze the gain for light that has traveled four times the length of the cavity, reflected three times internally, and exited through the front mirror. For a high finesse cavity such as ours, the shape of the cavity gain profile becomes a narrow Lorentzian centered about the cavity resonance ω_c:

$$g_{cav}(\omega) \approx \frac{const}{(\omega-\omega_c)^2 + \left[\frac{c^2(1-R^2)^2}{16R^2L^2}\right]} = \frac{const}{(\omega-\omega_c)^2 + (\frac{1}{2}\Gamma_c)^2} \tag{3}$$

where *const* is some normalization constant which can be determined by the given

parameters. This gives our cavity a natural linewidth of:

$$\Gamma_c = \frac{c}{4L}\frac{1-R^2}{R} = \frac{2\pi\nu_{FSR}}{F} \tag{4}$$

where $F = \pi R/(1-R^2)$ is the cavity finesse and $\nu_{FSR} = c/(4L)$ is the cavity free spectral range. These differ from the standard definitions of these terms for a planar cavity because the V-mode of our setup requires the laser light to travel twice the distance as in a standard planar-mirror cavity and reflects twice as many times.

For our cavity, we have a free spectral range of $\nu_{FSR} = 750$ MHz. Given the mirror reflectivities of our cavity, we can estimate an optimal finesse of:

$$F = \frac{2\pi}{l_{rt}} \approx \frac{2\pi}{2 \times 1.6\%} = 196 \tag{5}$$

where l_{rt} is the total round-trip loss, equal to twice the loss at the front mirror. This gives a nomimal cavity linewidth of $\Gamma_{opt} \approx 2\pi \times 3.8$ MHz. Our setup proves to be somewhat lossier than this ideal situation. From analysis of cavity transmission (see Figure 8 in Section 7), we calculated our cavity finesse to be approximately $F \approx 100$, which gives us a real cavity linewidth of $\Gamma_{cav} = 2\pi \times 7.5$ MHz.

When the resonant light from the cavity is fed back onto the laser diode, the cavity then becomes an extension of the passive optical feedback region of the laser diode but with much better selectivity than the Bragg reflector region of the laser diode. In addition to the cavity, we must also consider the path between the laser diode and the cavity in this feedback system. Similarly to the way the phase-controlled region of the DBR laser diode controls the coupling between the active region and the passive Bragg reflector region, the external path length controls the coupling between the laser diode and the external cavity. Optimum coupling of the cavity to the diode is achieved only when the path length is equal to an integrer number of wavelengths. Our method of achieving this is discussed further in Section 7. When resonant feedback is achieved, the wavelength of the laser diode is pulled to a resonant mode of the cavity, so the stability of the cavity's length is of vital importance. Our method of locking the cavity length is described further in Section 8.

5 Linewidth Reduction via Optical Feedback

In previous sections, we have discussed the gain profiles of both the laser diode medium and the external optical cavity. The laser diode's gain profile is approximately Lorentzian, with a width on the order of $\Gamma_L \approx 2\pi \times 10$MHz. Our optical

cavity's gain profile (Eq. 2) is also Lorentizian with a linewidth of $\Gamma_C \approx 2\pi \times 4$MHz. If we consider the two gain media to produce a single gain profile that is a product of the two, we find that the product of our two profiles is another Lorentzian with new linewidth of $\Gamma_N \approx 2\pi \times 3$ MHz. This small reduction in linewidth is significantly less than linewidth reductions reported from observations [8], so a simple linear model of optical gain from our cavity is inadequate.

Significant theoretical and experimental work has been done to explain and demonstrate laser linewidth reductions via external feedback [8, 9]. Olesen derives the formula for the the linewidth reduction factor:

$$\frac{\Delta\nu}{\Delta\nu_0} = \frac{1}{1 + \chi\sqrt{1+\alpha^2}} \tag{6}$$

Here α is a standard laser diode parameter known as the linewidth broadening factor [10] and is a factor intrinsic to the laser diode itself. The parameter χ is known as the feedback parameter [8] and is determined by external feedback.

The linewidth broadening factor α is defined as:

$$\alpha = -\frac{d[Re\{\chi_e(n)\}]/dn}{d[Im\{\chi_e(n)\}]/dn} \tag{7}$$

where n is the intrinsic carrier density and $\chi_e(n)$ is the susceptibility as a function of n [10]. For DFB diodes like our DBR laser diodes, this factor typically is in the range of $\alpha \sim 4 - 7$.

The feedback parameter χ is defined as:

$$\chi = \kappa\frac{\tau}{\tau_{in}} \tag{8}$$

where κ^2 is the ratio of power reflected from the external cavity relative to the power reflected from the laser mirror, τ is the total time spent in the external cavity, and τ_{in} the time spent in the laser diode cavity [8]. We can estimate values of these quantities for our experimental setup. We can break down the power ratio κ^2 into the fractional losses along the path to the cavity:

$$\begin{aligned}\kappa^2 &= (\frac{1}{2})(\text{pickoff})^2(\text{modematching})^2 \\ &= (0.05)^2(0.5)(0.30)^2\end{aligned} \tag{9}$$

where the amount of light isolated at the pickoff, is estimated to be approximately 5%; the modematching of light into the cavity is estimated to be optimally 30%; and

the factor of $1/2$ comes from the fact that half the laser power is lost in the other arm of the cavity V-mode. These two terms are squared in the above expression because the beam must return along the same path to return to the laser diode, so it is subject to the same losses twice. From the above expression, we determine a value for the power ratio of $\kappa \sim 10^{-2}$.

We can also estimate values for τ and τ_{in}. The laser diode cavity is very lossy, so we can estimate a photon traveling twice the length of the laser diode cavity L_{LDC} before exiting. Thus we calculate the total time spent in the laser diode cavity to be given by:

$$\tau = \frac{2L_{LDC}}{c} \approx \frac{2 \times 100\mu\text{m}}{3 \times 10^8\text{m/s}} = 6.7 \times 10^{-13}\text{s} \tag{10}$$

where we estimate the length of the laser diode cavity $L_{LDC} \approx 100\mu$m. For the time spent outside of the laser diode cavity, we estimate this as the lifetime of a photon in the external cavity:

$$\tau_{in} \approx \frac{1}{\Gamma_{cav}} = 1.3 \times 10^{-7}\text{s} \tag{11}$$

Thus we can determine a reasonable estimate of the feedback parameter χ for our experimental setup:

$$\chi = \kappa\frac{\tau}{\tau_{in}} \approx 2 \times 10^3 \tag{12}$$

From the above analysis, we can see that both α and χ are much larger than 1, so our equation for the linewidth reduction (Eq. 6) reduces to:

$$\frac{\Delta\nu}{\Delta\nu_0} \approx \frac{1}{\chi\alpha} = 10^{-4} \tag{13}$$

Thus we see from this analysis that the external feedback from our cavity should reduce our laser linewidth by four orders of magnitude.

6 Feedback Electronics

In our above discussions, we have already identified the need to electronically control two parameters: the path length between the laser diode and the external optical cavity, and the length of the cavity itself. Both control systems take as input a dispersive error signal, that is a signal with some slope that passes through zero at resonance. The error signal is then given some gain and fed back to a piezo to fix the piezo length to a lock point corresponding to zero error signal. The methods of obtaining the two error signals involve some interesting physics concepts and are

discussed in Sections 7 and 8. The system gain, however, must have the desired frequency response to effectively eliminate all mechanical noise as well as account for any mechanical resonances in the system.

The piezo itself has some capacitance, so the piezo in series with the output resistance of our feedback circuit acts as a frequency dependent voltage divider. This system, depicted in Figure 5a, has a gain profile given by:

$$G_1(\omega) = \frac{Z_C}{Z_R + Z_C} = \frac{1/i\omega C_P}{R_{out} + 1/i\omega C_P} = \frac{1}{1 + i\omega R_{out} C_P} \tag{14}$$

where R_{out} is the output resistance of our feedback circuit and C_P is the capacitance of the piezo. The Bode plot for this gain profile is labeled $G_1(\omega)$ in Figure 5c. The piezo system then has a corner frequency of $\omega_{c1} = (R_{out}C_P)^{-1}$ at which the system becomes an integrator. Due to more complicated structures of the piezo, its gain profile also has a second-order rolloff at a higher corner frequency ω_{c2}, after which the system behaves like a double-integrator.

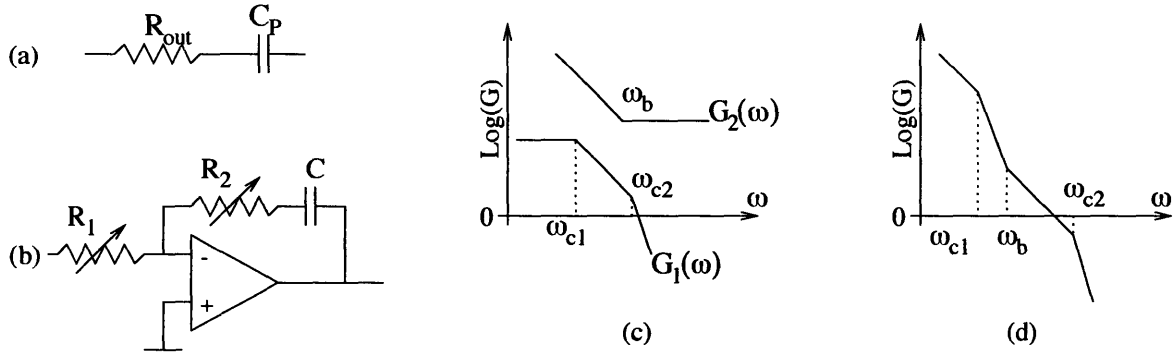

Figure 5: The two systems whose frequency responses are important are (a) the output-piezo voltage divider with gain profile $G_1(\omega)$ and corner frequency $\omega_{c1} = (R_{out}C_P)^{-1}$, and (b) the primary gain stage in the feedback circuit with gain profile $G_2(\omega)$ and corner frequency $\omega_b = (R_2C)^{-1}$. The gain plots are logarithmic Bode plots of (c) the piezo response $G_1(\omega)$ and programmable electronic response $G_2(\omega)$; and (d) the combined frequency response of the system $G_1(\omega) \times G_2(\omega)$.

The primary gain stage of our feedback circuit consists of an operational amplifier with input resistance R_1 and feedback impedence set by resistor R_2 in series with a capacitor C, as depicted in Figure 5b. This system has a gain profile described by

$$G_2(\omega) = \frac{Z_2}{Z_1} = \frac{R_2 + 1/i\omega C}{R_1} \tag{15}$$

The Bode plot for this gain profile is labeled $G_2(\omega)$ in Figure 5c, and we can see that the system has a corner frequency at $\omega_b = (R_2C)^{-1}$. At low frequencies the feedback impedence is dominated by the capacitor so the system acts like an integrator with gain that goes like $1/(\omega R_1 C)$, while at high frequencies the resistor dominates the feedback impedence so that the system has constant gain equal to R_2/R_1.

The total gain of the system is the product of the two gain profiles and the Bode plot, which is merely the sum of the previous two, is depicted in Figure 5d. From these plots we see that we can adjust the corner frequency of our feedback electronics by changing the value of R_2, and we can change the overall gain by changing R_1. We would like to increase the gain as much as possible to minimize excursions from the lock point arising from mechanical vibrations or thermal drift. However, we are limited by the requirement that the unity gain point cannot fall in a region where the system acts as a double integrator. This is because the double integrator has a phase of π (due to the $(i\omega)^{-2}$ factor), which means that the system will *amplify* any frequency with unity gain in a double integrator region. Thus we must adjust the gain carefully to ensure our system is stable.

7 Feedback Optimization: Path Length Lock

Optimum feedback from the cavity is achieved when the path length from the laser diode to the cavity is equal to an integer number of wavelengths of laser light. To monitor this path length, we must monitor the interference of the beam from the laser with the resonant cavity output. This is achieved by monitoring the second output beam of the cavity (the beam labeled (2) in Figure 6). This beam is an overlap of one of the resonant cavity output beams and a reflection of the incident beam from the laser diode. This achieves the interference we are seeking, but determining phase differences by monitoring the beat note of this beam is somewhat cumbersome.

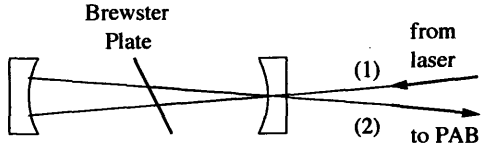

Figure 6: The two output beams from the cavity V-mode go to (1) the laser diode along the entry path and (2) to the polarization analysis box (PAB).

To acquire a more easily analyzable interference signal, we make use of a Brewster

plate within the cavity. The Brewster plate takes advantage of the differenct reflectivities for light polarized parallel or perpendicular to the plane of incidence (see Figure 7). For glass with index of refraction $n = 1.5$, the Brewster angle is $\theta_p = 56.1^o$. At this angle, the transmission coefficient for light polarized perpendicular to the plane of incidence is ≈ 1, while the transmission coefficient for light polarized parallel to the plane of incidence is $T \approx 0.86$. This means that every time the light passes through the Brewster plate, its component in the perpendicular direction experiences 14% loss. Our cavity has finesse of $F \approx 100$, so light traverses the cavity about 100 times before exiting, which means that light in the perpendicular direction is nearly completely eliminated.

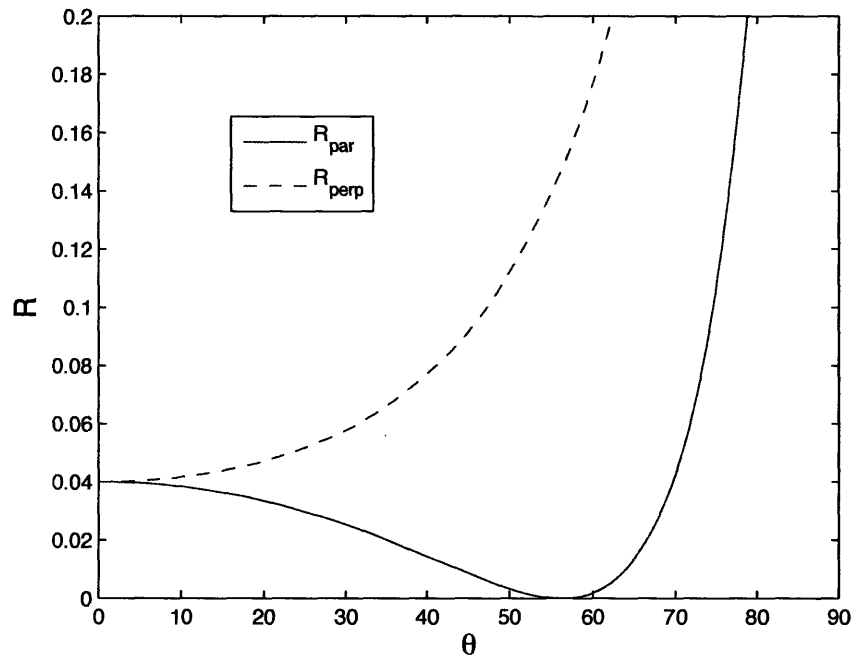

Figure 7: Reflection coefficients for light passing through n=1.5 glass at perpendicular incidence (solid) and parallel incidence (dashed).

We demonstrated this effect quantitatively by monitoring the cavity transmission for light polarized in each of the two primary directions. The solid curve in Figure 8 represents the cavity transmission for light oriented along the preferred axis of the Brewster plate, while the dotted curve is the cavity transmission for light with polarization perpendicular to the preferred axis of the Brewster plate. Both curves are plotted with the same scale, so it can clearly be seen that the transmission is

dramatically reduced in the dotted curve. This has the additional effect of reducing the effective finesse of the cavity to $F \approx 2$.

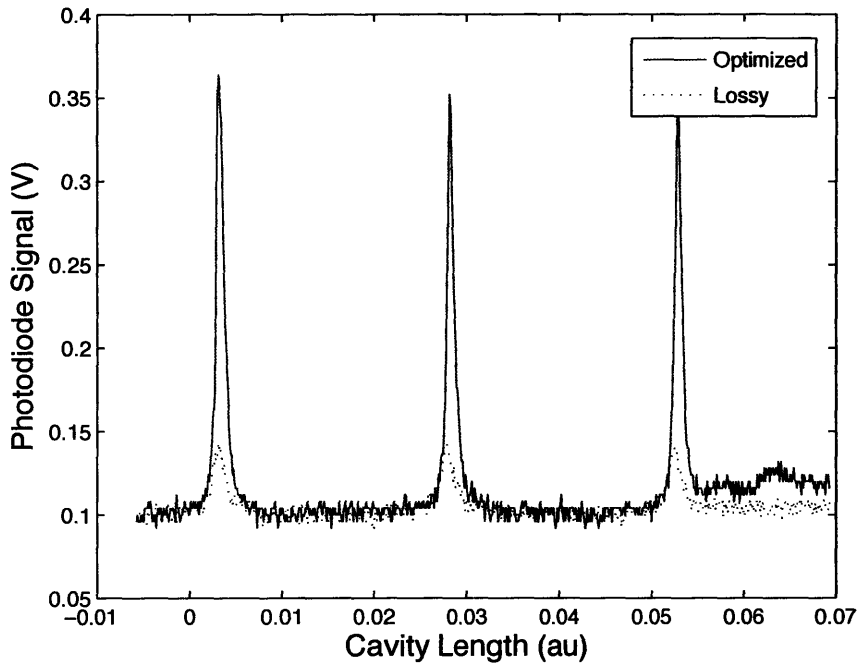

Figure 8: Cavity transmission for polarized light passing through the cavity with polarization direction parallel (solid curve) and perpendicular (dotted curve) to the maximum-transmission orientation of the Brewster plate.

Our method of locking the path length follows a clever scheme proposed by Hansch and Couillaud [1]. The beam incident to our polarization analysis box is a combination of the resonant cavity output, whose polarization has been pulled to that of the Brewster plate, and the laser diode light reflected off the surface of the front mirror of the cavity (see Figure 9a). When the path length is equal to an integral number of wavelengths, the two beams are in phase and their sum is simply a linear polarized wave whose polarization is a sum of the polarization of the two beams. If the path length is off resonance, however, the reflected beam acquires a phase shift associated with the phase offset of the path length. This results in an element of elliptical polarization in the beam going to the polarization analysis box. It is the presence of this elliptically polarized light that we want to detect with out polarization analysis box.

The PAB consists of a quarter-wave plate followed by a polarizing beams splitter

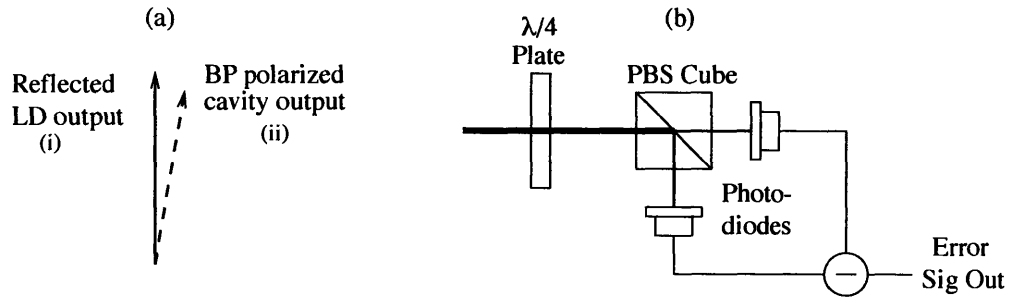

Figure 9: (a) Beam incident to polarization analysis box is combination of (i) laser diode light reflected off the front mirror surface and (ii) resonant output from the cavity whose polarization is pulled to that of the Brewster plate. (b) Light incident to polarization analysis box is sent through a $\lambda/4$ plate, and split onto two photodiode by a polarizing beam splitter (PBS) cube. The error signal is the difference of the two photodiode signals.

(PBS) cube, which splits light onto two photodiodes, and the difference between the two photodiodes is our error signal (see Figure 9b). Linear polarized light becomes circularly polarized by the $\lambda/4$ plate, so the light is split evenly by the PBS onto the two photodiodes and does not contribute to the error signal. Elliptically polarized light, however, is transformed into linearly polarized light by the $\lambda/4$ plate, so this light can be split unevely by the PBS cube and therefore generate an error signal. It is this error signal that is fed back to our locking electronics to adjust the path piezo so that the path length becomes an integer number of wavelengths long.

To determine the functional form of our error signal, let us again think of the path length between diode and cavity as another cavity by which the diode couples to the main cavity. If we call the total path length phase δ, then the signal from this cavity should be proportional to $1/(1 + A\sin^2\frac{1}{2}\delta)$, where $A = 4R/(1-R)^2$ is analogous to that from Eq. 2 but this time describes the reflectivities of the front face of the main cavity and the front face of the laser diode. The form of this coefficient is different as well because we consider the path length to act as a planar rather than spherical cavity. We also know that the error signal should be proportional to the path length difference from an integral number of wavelengths, so we can also say that the error signal should be proportional to $\sin\delta$. Thus we can establish an approximate functional form of our expected error signal:

$$Err(\delta) = \frac{\sin\delta}{1 + A\sin^2\frac{1}{2}\delta} \tag{16}$$

Note that this equation differs from the equation given by Hansch and Couillaud [1]. We chose not to use the functional given by Hansch because it gives infinite error signal values at $\delta = 0$, and so we felt did not accurately approximate what a real error signal would look like.

A graphical illustration of this theoretical model is depicted in Figure 10 with chosen $R \approx 0.50$. Real data was taken from our cavity setup by sweeping the path piezo and recording the error signal. The data for this is depicted in Figure 11. It is evident from our data that our error signal has a dispersive region to which we can lock the path length.

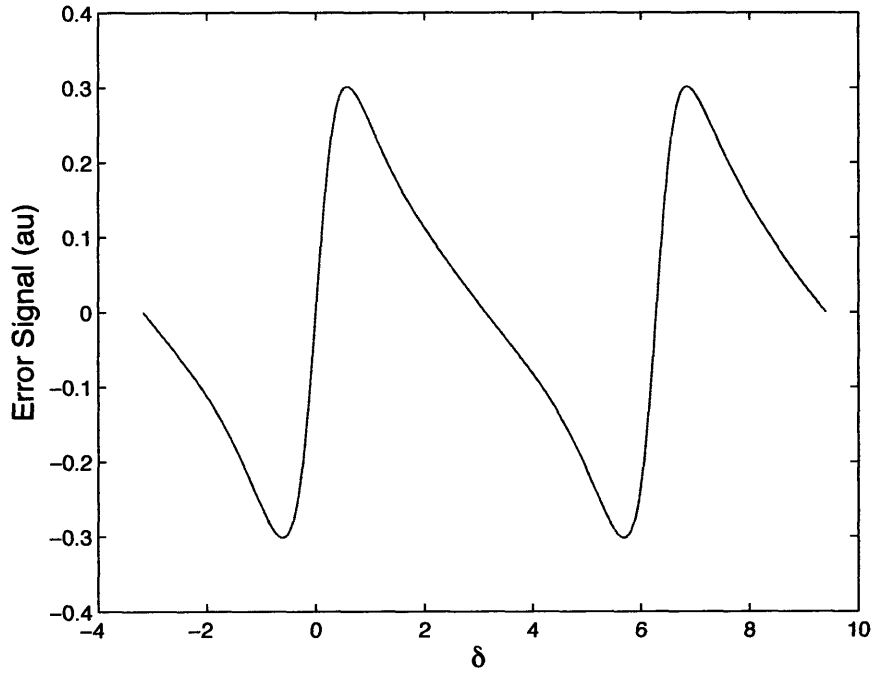

Figure 10: Theoretical path length error signal for $R \approx 0.50$.

8 Frequency Stabilization: Delay Line Lock

Once the feedback from the external optical cavity has been optimized, the laser's frequency is essentially locked to a resonant mode of the cavity, but this does not set the absolute frequency of the laser. The laser's frequency then is subject to the thermal drift of the cavity as well as mechanical noise, so an additional stage of

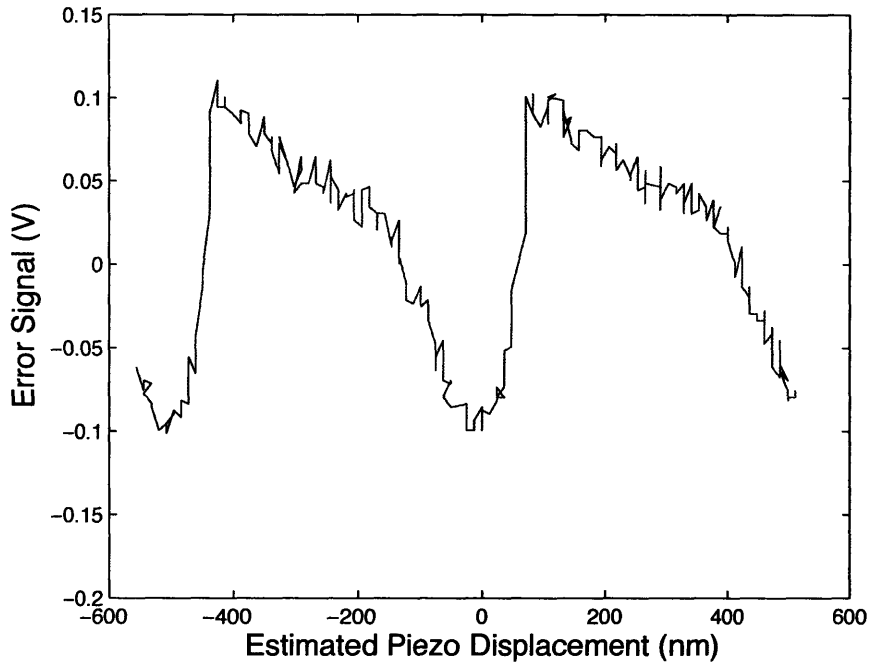

Figure 11: Real path length error signal from our cavity setup. Piezo displacement is estimated from conversion of piezo voltage using the piezo rating of $dL/dV \approx 60$ nm/V.

active feedback is necessary to maintain the laser at the desired frequency. This is done using a clever scheme devised by Schunemann et al [4] in which the beat note from the overlap of two lasers is used in conjunction with a delay cable to lock the difference frequency of the two lasers to some desired value. Our setup in fairly similar to that of Schunemann, and is depicted graphically in Figure 12.

The first stage of our locking system is the laser overlap section. Our narrow laser is overlapped with a reference laser whose frequency is locked to the 852.336 nm D-line of cesium. The wavelength of the narrow laser is monitored with a wavemeter and is brought to within a few picometers of the D-line wavelength. At this wavelength, the beat frequency f_b is related to the wavelength difference $\Delta\lambda$ by:

$$\frac{f_b}{\Delta\lambda} \approx 400\text{MHz/pm} \tag{17}$$

The typical bandwidth of standard commercial photodiodes is on the order of tens of kilohertz, so a special fast photodiode with bandwith of 20 GHz is needed to detect the laser beat note. A further concern with this setup is that the overlapped lasers

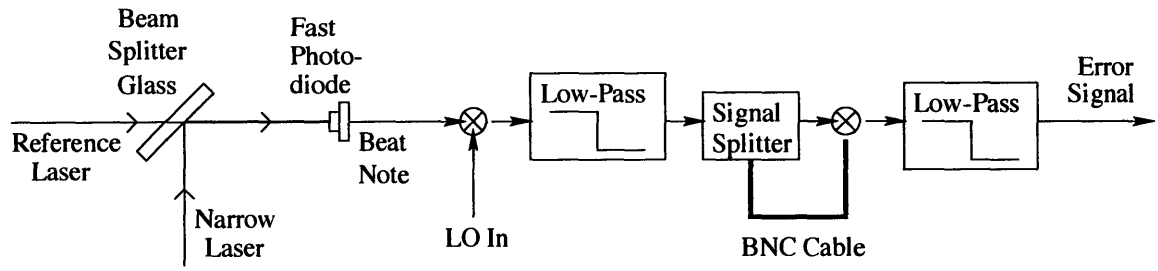

Figure 12: The beat note from the two lasers is detected on a fast photodiode then sent to a frequency mixer where it is mixed with a local oscillator (LO). This difference frequency is then split and send to a phase detector, where the phase introduced by the delay line acts as an error signal.

will produce a high frequency field as well. This field, whose frequency is the sum of the two laser frequencies, is too fast (at optical frequencies on the order of $\sim 10^{14}$ Hz) to be resolved by the photodiode. We therefore wish to isolate the AC signal from our photodiode, which correspondes to the beat note signal from the laser overlap. This is achieved by using a bias tee, which is depicted in Figure 13. The DC signal we do not want is removed along the inductor path while the desired AC signal containing the beat note is coupled out via the capacitor path and sent on to the next stage of the delay line lock.

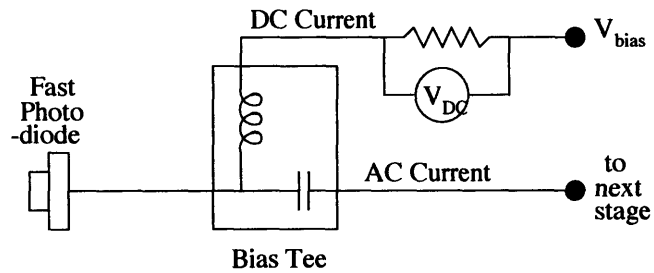

Figure 13: The DC signal is removed along the inductor path and monitored by measuring the voltage across the external resistor. The AC signal contains the desired beat note and is coupled out via the capacitor and then sent to the next stage of the delay line lock.

After isolating our optical beat note, we may wish to introduce some large frequency offset using a local oscillator (LO). This stage is not used in our current setup, but can be easily implemented. One particular reason this is useful is for driving tran-

sitions from specific hyperfine states, namely the $F = 4$ state which is separated from the $F = 3$ state by $f_{HF} = 9.192$ GHz [3]. This is particularly useful when driving Raman scattering processes between these two metastable ground states.. To add this offset stage to our setup, we combine the optical beat note with the local oscillator in a frequency mixer. The resultant output is the product of the two signals:

$$\cos(\omega_b) \cdot \cos(\omega_{LO}t) = \frac{1}{2}\cos(\omega_b + \omega_{LO})t + \frac{1}{2}\cos(\omega_b - \omega_{LO})t \tag{18}$$

We then send this signal through a low pass filter, which has the effect of removing the high frequency component (i.e. the $\cos(\omega_b + \omega_{LO})t$ term. We are then left with a purely sinusoidal signal whose frequecy we can label as the difference frequency $\omega_d = \omega_b - \omega_{LO}$.

After mixing our beat note with a local oscillator, we send the pure difference signal $x_d(t) = \cos(\omega_d t)$ to a signal splitter. One arm of the signal is sent along a delay line (i.e. a BNC cable about 1 m long) to a frequency mixer where it is mixed with the second arm of the signal which has no delay. The first signal acquires a phase θ along the delay line given by:

$$\theta = \omega_d L / v_s \tag{19}$$

where ω_d is the difference frequency, L is the length of the delay line, and v_s is the velocity at which the signal propagates along the BNC cable. The output of the frequency mixer then is the product of the original signal and the same signal with the delay line phase:

$$\cos(\omega_d) \cdot \cos(\omega_d t + \theta) = \frac{1}{2}\cos(\theta) + \frac{1}{2}\cos(2\omega_d t) \tag{20}$$

Passing this signal through a low pass filter isolates the term that is propotional to $\cos\theta$. The frequency mixer followed by the low pass filter acts as a phase detector, as depicted in Figure 12, yielding an error signal to which we can lock the frequency of our laser. Since θ is proportional to the difference frequency ω_d, we expect the error signal to be sinusoidal:

$$Err(\omega) = \cos(\omega_d L / v_s) \tag{21}$$

Data was taken for the error signal of our system at various beat note frequencies. The beat note frequency was determined by monitoring the photodiode output on a spectrum analyzer, while the error signal was monitored at the error output of our feedback circuit. The frequency of our laser was varied by changing the cavity length after locking the laser's frequency to the resonant cavity mode. Data for these measurements is presented in Figure 14.

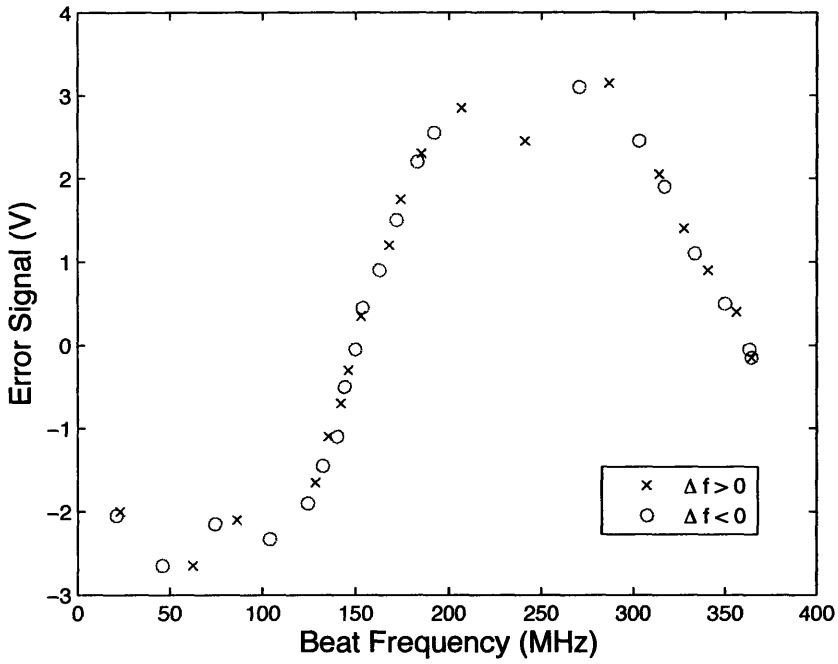

Figure 14: Error signal values for various beat note difference frequencies are plotted above. X-marks indicate "positive" difference frequencies while cirlce-marks indicate "negative" difference frequencies.

Note that data is plotted for difference frequencies that are "positive" (indicated by x-marks) and "negative" (indicated by circles). By "positive" and "negative" we mean that to go between these two regimes we decrease the difference frequency until it passes through zero and then increases with constant direction of piezo tuning. One clearly visible result is that our data is consistent on both sides of the error signal zero, and that the error signal does seem to be sinusoidal with maximum magnitude near zero.

Another visible consequence of our data is that we cannot lock to zero offset frequency. As stated in Section 6, we need an error signal that has some slope and passes through zero. We therefore lock our beat note to an offset frequency of about 300-400 MHz, with locked error signal magnitude limited to $|Err| \leq 20$ mV. Using the sinusoidal model of Eq. 21 with amplitude $A \approx 3$ V and period $\tau \approx 300$ MHz, we can calculate that our laser frequency is stable to within $|\Delta f| \leq 300$ kHz.

8.1 Thermal Expansion

An issue of major concern in this system is the thermal expansion of the cavity. Fixing the laser's frequency by locking the cavity length is impossible if the cavity expands beyond the range of tunability of the piezo. The typical piezo expansion for our system is $dL/dV = 2.1$ nm/V, with a total voltage range of about 280 V, giving a total piezo tuning range of $\Delta L_{max} = 588$ nm. Tuning the cavity length by $\lambda/4 = 213$ nm is equivalent to sweeping one free spectral range, so the cavity range in terms of free spectral range tunability is $\Delta f_{cav}/\nu_{FSR} = 2.76$.

An earlier version of this apparatus used a copper cavity, which has a thermal expansion coefficient of $\alpha_{Cu} = 19 \times 10^{-6}$ K^{-1}. For the cavity to expand beyond the piezo tunability range, this translates into a temperature change of $\Delta T = 0.31$ K. Since we want to account for temperature drifts in the lab of up to ≈ 5 K, this cavity was highly unstable.

To correct this problem, we specially ordered a custom-manufactured tube of Ultra-Low-Expansion (ULE) glass, whose expansion coefficient is nominally $\alpha_U \approx 0.1 \times 10^{-6}$ K^{-1} at 25^{o}C. The piezo in the cavity has an expansion coefficient of $\alpha_p = 3.7 \times 10^{-6}$ K^{-1} and a length of $L_p = 1.25$ cm. Combined with the ULE tube of length $L_U = 8.75$ cm this gives the entire cavity an ideal expansion coefficient of $\alpha_{cav} = 0.55 \times 10^{-6}$ K^{-1}, making the limiting temperature range for stability $\Delta T \approx 11$ K, which is well within the range of temperature drifts in the lab.

In the real cavity the thermal expansion matched closely to the theoretical calculations. We heated and cooled the cavity while monitoring the cavity transmission. To obtain the most accurate measurements, we held the cavity at a high temperature and allowed it to thermally equilibrate, then allowed it to cool and held it at a low temperature. After multiple iterations of this procedure, it was discovered that the cavity drifted by one free spectral range over a temperature change of $\approx 4K$. This means the experimental range of temperatures over which we can stabilize the laser frequency has a magnitude of $\Delta T \approx 11K$, which again is well within experimental control.

9 Applications of the Narrow Laser

Now that we have developed a basic understanding of cavity dynamics and have demonstrated the construction of a narrow frequency-band laser, we can discuss po-

tential applications of this technology.

9.1 Single Atom Detection in an Optical Cavity

Let us consider a single stationary cesium atom of diameter d in an optical cavity of length L, as depicted in Figure 15. Suppose we are passing light through the cavity such that the light is resonant with the atom and slightly off resonant with the cavity. This resonant laser light is affected by the presence of the atom because the atom has a different index of refraction than the vacuum, and let us call the atom's refractive index n_a.

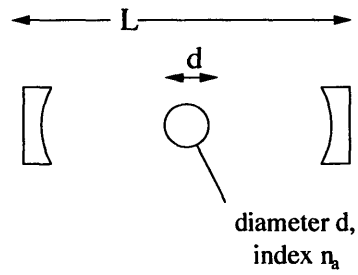

Figure 15: An atom of diameter d with refractive index n_a in a cavity of length L changes the effective length of the cavity.

This has the effect of altering the effective optical length of the cavity:

$$L_{eff} = L + (n_a - 1)d = L + \Delta L \tag{22}$$

and this in turn shifts the cavity resonance. If we recall Eq. 2, we see that we can solve for the new cavity resonance by keeping constant the term:

$$\omega L = (\omega + \Delta\omega) \cdot (L + \Delta L) \approx \omega\Delta L + L\Delta\omega \tag{23}$$

Combining this result with our expression for the cavity length shift given in Eq. 22 we see the shift in the cavity resonance is:

$$\Delta\omega = -\omega(n_a - 1)d/L \tag{24}$$

For optical frequencies of order $\omega \sim 10^{15}$Hz, atomic lengths of order $d \sim 10^{-10}$m and index of refraction shifts of order $(n_a - 1) \sim 1$ we see that the cavity resonance shifts by only a few hundred kilohertz. This value is much smaller than the linewidth of our

optical cavity or the linewidth of a broad frequency-band laser. From this order-of-magnitude calculation alone we can see the necessity of having a narrow frequency-band laser for such detection experiments, because the presence of an atom would not cause a cavity shift noticeable with a broad band laser.

Let us now consider how we might use a narrow frequency band laser to detect an atom in an optical cavity. If we again consider light that is resonant with the optical cavity of length L, but this time with a narrow laser with linewidth of order $\Gamma_L \sim 10\text{kHz}$. The spectrum of the cavity output then is a product of the frequency distribution of the laser, which we assume is Lorentizian about some center frequency ω_L with linewidth Γ_L, and the cavity gain function given in Eq. 2. Since the laser linewidth is several orders of magnitude smaller than the linewidth of the optical cavity, we can treat the laser distribution effectively as a delta function in frequency space. The cavity output then will be the value of the cavity gain at the laser frequency ω_L.

Now let us recall the situation described above, where an atom in an optical cavity changes the effective length of the cavity. Since the variable quantity here is the cavity length, it is useful to rewrite the cavity gain profile as a function of the length L and approximate it as a Lorentzian centered about resonant cavity length L_0:

$$G(L) = \frac{a^2}{a^2 + (L - L_0)^2}; \quad a = \frac{(1 - R^2)c}{4R\omega} \tag{25}$$

We now want to place an atom in our optical cavity and measure the change in the cavity output due to the presence of the atom. To maximize the signal change, we choose to set our initial cavity length L_i such that the cavity output is half its maximum value, $G(L_i) = 1/2$, which also yields the condition $L_i - L_0 = a$. We can evaluate the slope of the gain profile at this point by Taylor expanding to first order:

$$\frac{\partial G(L)}{\partial L} = \frac{-2a^2(L - L_0)}{(a^2 + (L - L_0)^2)^2} = \frac{-2(L - L_0)}{a^2} G^2(L) \tag{26}$$

Thus for a small length change ΔL about the initial length L_i we can find the first order output shift ΔG by substituting $G(L_i) = 1/2$ and $L_i - L_0 = a$ to obtain:

$$\Delta G = \frac{\partial G(L)}{\partial L} \Delta L = -\frac{1}{2a} = -\frac{\Delta L}{\lambda} \frac{4\pi R}{1 - R^2} \tag{27}$$

We can then evaluate this quantity for a cavity with reflection coefficients equal to those of our above cavity, laser light of wavelength $\lambda = 852$ nm, and cavity length shift $\Delta L \sim d \sim 10^{-10}\text{m}$. We obtain a first order correction of $\Delta G = -0.046$. Such

a large fractional signal change should be detectable on a photodiode placed at the cavity output, so long as the noise level is significantly smaller than this signal change. Thus we have illustrated how a narrow laser allows for atom detection that would not be possible with a standard broad laser.

Acknowledgments

The author is grateful to Vladan Vuletic, James K. Thompson, Adam Black, and Jonathan Simon at MIT's Center for Ultracold Atoms, whose expertise in this field greatly aided the author's understanding of and ability to write about this subject.

References

[1] T.W. Hansch and B. Couillaud, "Laser frequency stabilization by polarization spectroscopy of a reflecting reference cavity." Optics Communications 35:441 (1980).

[2] B. Dahmani, L. Hollberg, and R. Drullinger, "Frequency stabilization of semiconductor lasers by resonant optical feedback." Optics Letters 12:876 (1987).

[3] D.A. Steck, "Cesium D Line Data." Los Alamos National Laboratory (unpublished) (2003).

[4] U. Schunemann et al, "Simple scheme for tunable frequency offset locking of two lasers." Review of Scientific Instruments 70:242 (1999).

[5] H. Ghafouri-Shiraz, *Distributed Feedback Laser Diode and Optical Tunable Filters* (John Wiley and Sons, West Sussex, England, 2003), chapter 10.

[6] C.S. Adams and E. Riis, "Laser Cooling and Trapping of Neutral Atoms." Progress in Quantum Electronics 21:1.

[7] J.M. Vaughan, *The Fabry-Perot Interferometer* (Adam Hilger, West Sussex, 1989).

[8] H. Olesen, J.H. Osmundsen, and B. Tromborg, "Nonlinear dynamics and spectral behavior for an external cavity laser." IEEE Journal of Quantum Electronics 22:762 (1986).

[9] R. Lang and K. Kobayashi, "External optical feedback effects on semiconductor injection laser properties." IEEE Journal of Quantum Electronics 16:347 (1980).

[10] M. Osinski and J. Buus, "Linewidth broadening factor in semiconductor lasers - an overview." IEEE Journal of Quantum Electronics 23:9 (1987).